

# Effect of Temperature on Athabasca Type Heavy Oil – Water Relative Permeability Curves in Glass Bead Packs

Mohammad Ashrafi<sup>1</sup>, Yaser Souraki<sup>1</sup> & Ole Torsaeter<sup>1</sup>

<sup>1</sup> Department of Petroleum Engineering and Applied Geophysics, Norwegian University of Science and Technology – NTNU, Trondheim, Norway

Correspondence: Mohammad Ashrafi, Department of Petroleum Engineering and Applied Geophysics, Norwegian University of Science and Technology – NTNU, S.P. Andersens vei 15A, 7491 Trondheim, Norway. Tel: 47-73-591-117. E-mail: mohammad.ashrafi@ntnu.no

Received: August 28, 2012 Accepted: September 14, 2012 Online Published: October 14, 2012

doi:10.5539/eer.v2n2p113

URL: <http://dx.doi.org/10.5539/eer.v2n2p113>

## Abstract

There have been a number of somehow contradictory reports in the literature on the effect of temperature on oil and water relative permeabilities. Although some authors have reported the dependence of relative permeability curves on temperature, others have attributed these dependencies to artifacts inherent in unsteady-state method of relative permeability measurement. In order to further investigate the impact of temperature changes on the relative permeability data, we have conducted laboratory core flooding experiments on heavy oil systems. The porous media used was glass bead packs, and the Athabasca type bitumen with varying viscosities was displaced by hot water. The history matching technique was conducted on production and pressure differential data to get the relative permeability curves.

Results indicated that generally the increase in initial water saturation and the decrease in residual oil saturation are expected by increasing temperature. However, viscous instabilities can rule out the above mentioned trends. No temperature dependency of either oil or water relative permeability can be justified in our tests. The changes in relative permeabilities by temperature are probably related to experimental artifacts, viscous fingering and changes in oil to water viscosity ratio and not fundamental flow properties.

**Keywords:** relative permeability, unsteady-state method, history matching, end point saturations, heavy oil, viscosity

## Nomenclature

### Symbols

BPR	Back Pressure Regulator	GB	Glass Beads
HT	High Temperature	JBN	Johnson, Bossler and Naumann technique
$k_r$	Relative Permeability	LT	Low Temperature
PV	Pore Volume	$S_{wi}$	Initial Water Saturation
$S_{or}$	Residual Oil Saturation	SAGD	Steam Assisted Gravity Drainage
SCAL	Special Core Analysis	$T$	Absolute Temperature, K
$\mu$	Dynamic Viscosity, cP		

### Subscripts

$o$	Oil	$w$	Water
-----	-----	-----	-------

### Superscript

$0$	End Point Value	$*$	Normalized Value
-----	-----------------	-----	------------------

## 1. Introduction

The modeling of heavy oil production by thermal methods requires an in depth understanding of the rock-fluid interaction parameters for these types of reservoirs. The multi phase flow parameters are also crucial for modeling and evaluating the production mechanisms in these types of reservoirs. An important multi phase flow

parameter is relative permeability. Relative permeability is the ratio of the effective permeability of a fluid at a given saturation to that at 100% saturation (Amyx, 1960). Wettability changes resulted from temperature increase, have an impact on the relative permeability. Viscosity is also governed by temperature, and will have important effects on the relative permeability. There are generally two methods of measuring relative permeabilities, namely steady state and unsteady state methods. Both methods have been used in the literature to study the effect of temperature on the relative permeability curves. Looking back in to the literature we can find some contradictory reports on the effect of temperature on the relative permeability ( $k_r$ ) curves. Some authors have reported an increase in the irreducible water saturation ( $S_{wi}$ ) and a decrease in residual oil saturation ( $S_{or}$ ) as the temperature of the system increases. This shift in the saturations results in some changes in the value of  $k_r$  as well. There are some reports showing that the value of oil relative permeability ( $k_{ro}$ ) increases while the value of water relative permeability ( $k_{rw}$ ) decreases at higher temperatures. The effect of temperature on the end point saturations ( $S_{wi}$  and  $S_{or}$ ) has been reported by several authors (Edmondson, 1965; Combarous & Pavan, 1968; Poston et al., 1970; Sinnokrot, 1971; Lo & Mungan, 1973; Weinbrandt et al., 1975; Abasov et al., 1976; Maini & Batycky, 1985; Torabzadeh & Handy, 1984; Bennion et al., 1985). All these authors except Combarous and Pavan (1968) have also reported the change of  $k_r$  curves with temperature. Davidson (1969) has indicated the effect of temperature on the relative permeability, while not mentioning anything about the end point saturations. Maini and Okazawa (1987) have considered fixed end point saturations and have confirmed the change in  $k_r$  values with temperature. Schembre et al. (2006) have proposed that the rock becomes more water wet at higher temperatures and that affects the relative permeability curves. On the other hand, there are some results published in the literature confirming no effect of temperature neither on the relative permeability nor on the end point saturations (Wilson, 1956; Sufi et al., 1982; Miller & Ramey, 1985). The two latter have concluded that the previously reported temperature dependant behaviors of relative permeability and residual saturations might have been affected by viscous instabilities, capillary end effects and / or difficulties in maintaining material balance (Polikar et al., 1990).

Besides these variations in the reported results, there are very few experimental studies specifically done on bitumen reservoirs of Alberta. Poston et al. (1970) worked on very viscous oils and reported the changes of both residual saturations and relative permeability values. Maini and Batycky (1985) have also conducted their experiments on heavy oil and indicated the variations with temperature except for the  $k_{rw}$ . Polikar et al. (1990) worked specifically with Athabasca type bitumen and proposed no dependency on temperature. Sedaei Sola et al. (2007) have performed some experiments using heavy oil and reported dependencies on temperature.

Researchers have used both mineral and crude oil in their studies. Some studies have been done on consolidated core samples while others have used unconsolidated material like sand packs or glass beads. These variations in the experimental conditions have resulted in different and even contradictory results. This implies that the actual effect of temperature on flow behavior of fluids in the rock is case specific.

Due to the contradictory reports and conclusions, which are because of variation in the systems being tested, it seemed necessary to conduct our own core flooding experiments and investigate the dependency of relative permeability curves on temperature. The objective was accomplished by performing core flooding experiments, displacing heavy oil by hot water at different temperatures and using oils with varying viscosities. The production curves and pressure differential data in each experiment were history matched to get the oil and water relative permeabilities.

## 2. Relative Permeability Calculation Method

There are generally two methods of relative permeability measurement in the oil industry, namely steady-state and unsteady-state. In steady-state technique, a fixed ratio of two immiscible fluids are mixed and injected simultaneously into the porous media until saturation and pressure equilibria are reached. A faster method is unsteady-state technique, which is based on the displacement of one fluid phase by another immiscible fluid phase (Honarpour et al., 1986). In this study we only conduct unsteady-state or displacement method. Relative permeabilities can be calculated from recorded production and pressure differential data of a displacement test. This can be done by either explicit or implicit calculation. The explicit methods mostly used are the JBN (Johnson, Bossler, & Naumann) technique (Johnson et al., 1959) and its modified version by Jones and Roszelle (1978). The implicit method or history matching is, however, based on numerical calculation. The relative permeability parameters are adjusted to match the production and pressure differential data from core flooding experiments (Wang et al., 2006). The history matching of data was done using a core flooding simulator called Sendra. This software is a two-phase 1D black-oil simulation model used for analyzing SCAL (special core analysis) experiments. It is tailor made for revealing relative permeability and capillary pressure from two-phase and multi-phase flow experiments performed in the SCAL laboratory (Sendra user guide, 2012). This software

acts as both a core flooding simulator and a history matching tool. Through history matching function, one can match the experimental data by adjusting the relative permeability curves. This is done by choosing the appropriate relative permeability correlation in the simulator. The software is then varying the empirical parameters in the function trying to match the experimental data. For the estimation method used in Sendra, refer to the software manual (Sendra user guide, 2012). There are several relative permeability correlations included in this simulator. Below is a review of these correlations. The normalized water saturation is used in all correlations:

$$S_w^* = \frac{S_w - S_{wi}}{1 - S_{wi} - S_{or}} \quad (1)$$

For simplicity, the formulations are given for oil-water systems; however they behave similar for oil-gas and water-gas systems (Sendra user guide, 2012).

### 2.1 Burdine Correlation (Burdine, 1953)

$$k_{rw} = k_{rw}^0 \left( S_w^* \right)^{\frac{2+3\lambda}{\lambda}} \quad (2)$$

$$k_{ro} = k_{ro}^0 \left( 1 - S_w^* \right)^2 \left( 1 - \left( 1 - S_w^* \right)^{\frac{2+\lambda}{\lambda}} \right) \quad (3)$$

### 2.2 Corey Correlation (Corey, 1954)

$$k_{rw} = k_{rw}^0 \left( S_w^* \right)^{N_w} \quad (4)$$

$$k_{ro} = k_{ro}^0 \left( 1 - S_w^* \right)^{N_o} \quad (5)$$

### 2.3 Sigmund & McCaffery Correlation (Sigmund & McCaffery, 1979)

$$k_{rw} = k_{rw}^0 \frac{\left( S_w^* \right)^{N_w} + A S_w^*}{1 + A} \quad (6)$$

$$k_{ro} = k_{ro}^0 \frac{\left( 1 - S_w^* \right)^{N_o} + B \left( 1 - S_w^* \right)}{1 + B} \quad (7)$$

### 2.4 Chierici Correlation (Chierici, 1984)

$$k_{rw} = k_{rw} \left( S_{or} \right) e^{-BR_w^M} \quad (8)$$

$$k_{ro} = k_{ro} \left( S_{wi} \right) e^{-AR_w^L} \quad (9)$$

$$R_w \left( S_w \right) = \frac{S_w - S_{wi}}{1 - S_{or} - S_w} \quad (10)$$

### 2.5 LET Correlation (Lomeland et al., 2005)

$$k_{rw} = k_{rw}^0 \frac{\left( S_w^* \right)^{L_w}}{\left( S_w^* \right)^{L_w} + E_w \left( 1 - S_w^* \right)^{T_w}} \quad (11)$$

$$k_{ro} = k_{ro}^0 \frac{(1 - S_w^*)^{L_o}}{(1 - S_w^*)^{L_o} + E_o (S_w^*)^{T_o}} \quad (12)$$

For the analysis of data in this study, all the above mentioned correlations have been tried to get the best possible history matching of the experimental data.

### 3. Experimental Procedure

#### 3.1 Relative Permeability Measurement Set-up

The flooding set-up used in this study is shown in Figure 1. A core holder is placed in an oven that can be set at any desired temperature up to 300°C. The oven is equipped with window panels and two fans which help to provide a constant temperature by circulating the air inside the oven. End caps of the core holder were designed in such a way that the fluid could be distributed evenly at the injection face. The overburden pressure is provided by viscous paraffin which has a viscosity of around 120 cp at room temperature and is contained in a cylinder with a floating piston. A Quizix positive displacement pump provides the pressure behind the piston using distilled water. This pump can be set to operate at a constant pressure by either displacing or recovering the water. This makes it possible to keep a constant overburden pressure by recovering the extra paraffin due to expansion at higher temperatures inside the oven. A pressure gauge placed on the paraffin line shows the pressure, and is visible through the windows of the oven. Two other pressured vessels are used in order to inject the water or oil alternatively. These two cylinders are also equipped with floating type pistons. The pistons are displaced by distilled water using another Quizix pump that operates at constant rate. The pump's operational range is 0.001 cc/min up to 50 cc/min. A back pressure regulator (BPR) is set inside the oven on the production line. This BPR is used to provide a higher pressure than the atmospheric pressure inside the system to make sure the water is in the liquid phase. A glass tube separator is placed outside the oven. The effluent enters the separator, which is filled with water, at the bottom. The oil phase is gathered on top and the water leaves to another BPR. The produced water is accumulated on a scale. Pressure differential across the core is monitored using a Keller pressure transducer with a 0-3 bar operation range. The transducer is connected to a PC to have a continuous pressure reading.

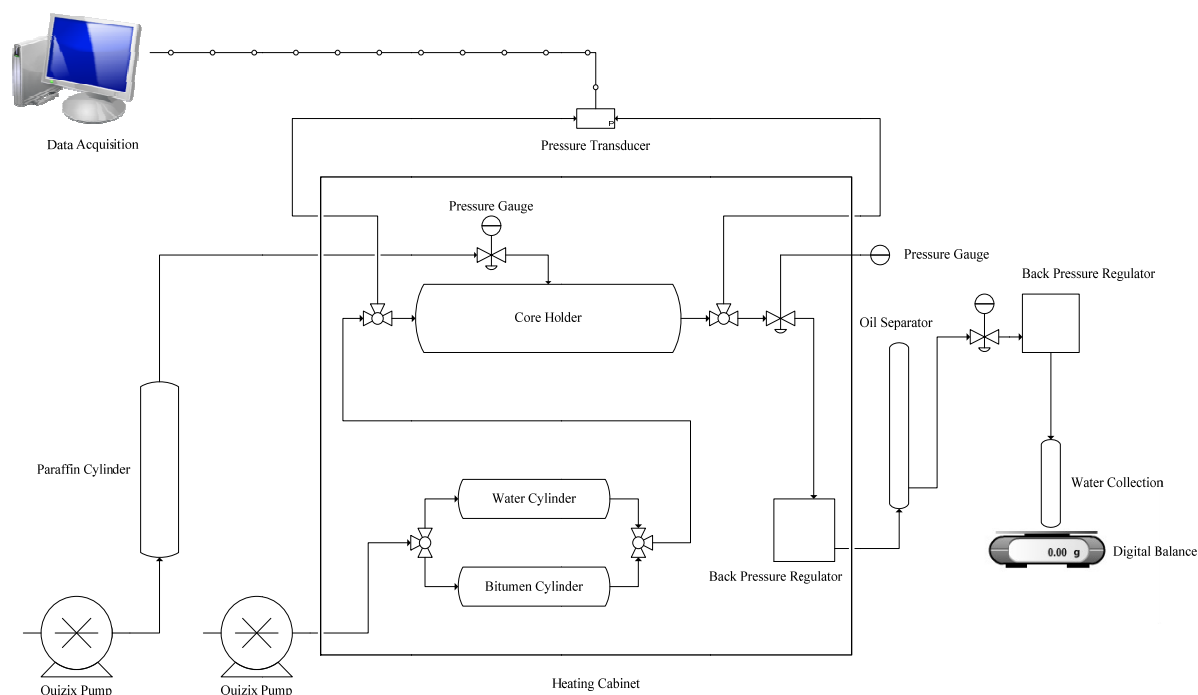


Figure 1. Schematic representation of core flooding setup used in this study

### 3.2 Porous Media and Packing Procedure

The porous media used was unconsolidated glass beads. Glass beads of different size were packed inside a rubber sleeve. Two metal screens were placed on the top and bottom of the packed media inside the sleeve and in contact with end caps of core holder. These screens were used to obviously prevent the production or any movement of glass beads and at the same time evenly distribute the fluid at the injection port. The rubber sleeve was installed on the inlet end cap, and the metal screen was placed inside and in contact with the end cap face. They were then placed on an electric shaker. While the shaker was running the glass beads were poured using a funnel until having a pack of desired length. The same packing procedure was always used to make sure we have a homogeneous medium. The diameter of the pack was 3.8 cm and the length was 21 cm.

### 3.3 Procedure

The packed porous media was installed inside the core holder. After providing the overburden pressure of 25 bars, the packed porous media was saturated with distilled water using a vacuum pump. The porosity of the pack was calculated by doing a material balance on the amount of water left and knowing the exact value of the dead volume of lines connected to the core. The absolute permeability of the packed core was measured vertically using an accurate pressure transducer with an operational range of 0-3 bars. The core holder was then placed inside the oven in horizontal position, and water injection was performed until reaching the desired temperature and pressure inside the core. In the next step, oil was injected at a rate of 0.5 cc/min to initialize the core and calculate the initial water saturation ( $S_{wi}$ ). Oil injection was continued at  $S_{wi}$  to measure effective oil permeability. After initializing the core, the separator was connected and the imbibitions process was initiated by injecting water at a rate of 0.8 cc/min. This rate was even less than 1 PV/h as recommended by Polikar et al. (1990). During the water injection phase, the oil production was recorded versus time, and the pressure differential across the core was monitored as well. The water injection was continued for almost 20 hours. After the experiment, the separator was disconnected and held at a temperature of 40°C for a few days in order for the oil/water meniscus to be separated completely and any possible adjustment to the final oil recovery.

### 3.4 Oil Preparation and Viscosity Measurement

The type of oil used in this study was a blend of Athabasca bitumen and n-dodecane. The bitumen sample used is obtained from an oil sand reservoir in Athabasca region, produced using SAGD method. The sample has not been exposed to any solvent and the condensed water produced together with the bitumen has been removed at high temperature. The viscosity, density, molecular weight and some other PVT properties of Athabasca bitumen were measured as highlighted in Ashrafi et al. (2011). Bitumen was added to n-dodecane in known amounts, and the mixture was stirred on a magnetic stirrer. Two types of oil were prepared by mixing bitumen with 10% n-C<sub>12</sub> added and 20% n-C<sub>12</sub> added on a mass basis. These oils are referred to as OIL10 and OIL20. The properties of bitumen and these two oils are shown in Table 1.

Table 1. Oil properties

Component	Molecular Weight (g/gmole)	Density (g/cc)
Athabasca bitumen	534	1.0129
n-dodecane (n-C <sub>12</sub> )	170.34	0.748
OIL10	440.1	0.9783
OIL20	374.2	0.9459

The viscosities of these two oils are also measured using a digital rotational viscometer as done for Athabasca bitumen (Ashrafi et al., 2011). The viscosity measurements were done in 10 °C intervals, allowing sufficient time at each temperature step to have a reasonable viscosity reading. For pure Athabasca bitumen the measurements were done from room temperature up to 300 °C. While for OIL10 and OIL20, the measurements were done up to 70 °C and extrapolated for higher temperature values. This was due to the possibility of n-dodecane evaporation at higher temperatures. The extrapolation was done using an empirical equation for the viscosity of gas free Athabasca bitumen presented by Khan et al. (1984). This equation is as follows:

$$\ln \ln(\mu) = c_1 \ln T + c_2 \quad (13)$$

In this equation  $\mu$  is dynamic viscosity of heavy oil sample in “mPa.s” or “cp”, at atmospheric pressure and

temperature  $T$  (K). The constants  $c_1$  and  $c_2$  are empirical and can be found for each sample using experimental data. They can be determined using the least square parameter estimation technique. The applicability of this equation to our bitumen sample was tested and compared with the data provided by Khan et al. (1984) and Ashrafi et al. (2011). The values of empirical constants  $c_1$  and  $c_2$  for the bitumen, OIL10 and OIL20 are presented in Table 2. The viscosity versus temperature curve is also shown in Figure 2.

Table 2. Empirical constants of equation (13) for Athabasca bitumen, OIL10 and OIL20

Component	$c_1$	$c_2$
Athabasca bitumen	-3.5912	22.976
OIL10	-3.4563	21.872
OIL20	-3.5094	21.905

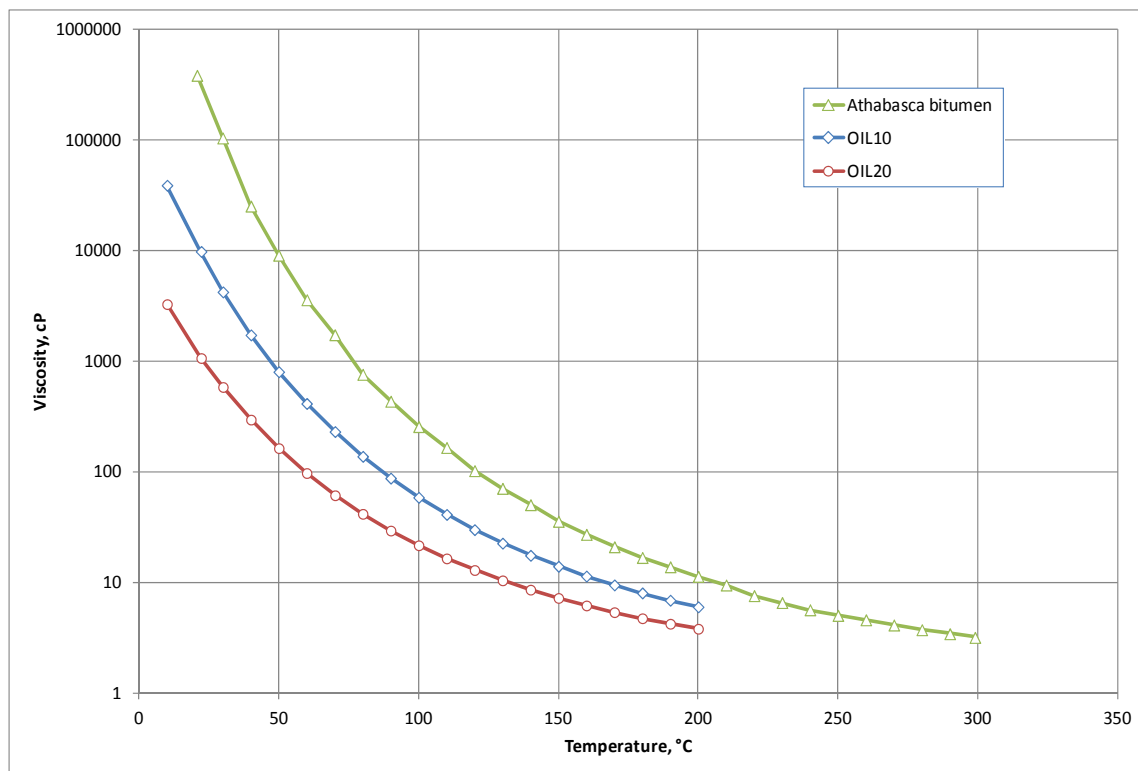


Figure 2. Viscosity of Athabasca bitumen, OIL10 and OIL20 versus temperature

#### 4. Results and Discussion

The porous media used in this study were artificial core plugs made of glass beads (GB) packed inside the rubber sleeve. Two sizes of glass beads were used, 1 millimeter size and 300-425 micron size beads. The absolute permeabilities of cores were measured by injecting water vertically upwards. The absolute permeability was, however, used as an adjusting parameter in simulations by Sendra to match the experimental pressure drop observed. An overview of experimental parameters is listed in Table 3.

Table 3. Experimental conditions

Core properties	
Length	21 cm
Diameter	3.8 cm
Permeability (1mm size GBs packs)	90 to 100 Darcies
Permeability (300-425 micron GBs packs)	40 to 45 Darcies
Flooding Conditions	
System pressure	5 bars
Overburden pressure	25 bars
Oil injection rate	0.5 cc/min

Different sets of experiments were run on glass bead packs. These flooding experiments were designed to examine the effect of various parameters on flow behavior and relative permeability curves. Table 4 summarizes the experiments performed during this study.

Table 4. Experiments performed during this study

Porous Media	Experiment Type	Temperature °C	Oil Type	Injection rate cc/min	Porosity %	Pore volume cc	S <sub>wi</sub> %
1 mm GBs	LT*	50	OIL20	1	29.01	69.1	20.98
		70	OIL20	1	28.80	68.6	17.49
	HT**	100	OIL20	1	30.06	71.6	19.55
		120	OIL20	1	30.06	71.6	16.76
		120	OIL20	0.8	30.27	72.1	15.95
		140	OIL20	0.8	30.90	73.6	16.30
		100	OIL10	0.8	31.95	76.1	11.83
		120	OIL10	0.8	31.53	75.1	21.30
		140	OIL10	0.8	31.32	74.6	28.15
		100	OIL20	0.8	32.37	77.1	11.02
		120	OIL20	0.8	33.21	79.1	13.91
300-425 micron GBs	HT	140	OIL20	0.8	32.79	78.1	21.13
		100	OIL10	0.8	33.84	80.6	14.02
		120	OIL10	0.8	34.26	81.6	13.48
		140	OIL10	0.8	34.05	81.1	17.88

\* Low temperature experiments

\*\* High temperature experiments

As mentioned earlier, the method of relative permeability calculation was history matching the production curve and pressure differential data using Sendra simulator. Different relative permeability correlations were used, and the parameter estimation was done by the software to get the best match. Figure 3 shows the pressure differential match and production curve match for LT experiment at 70°C as an example.

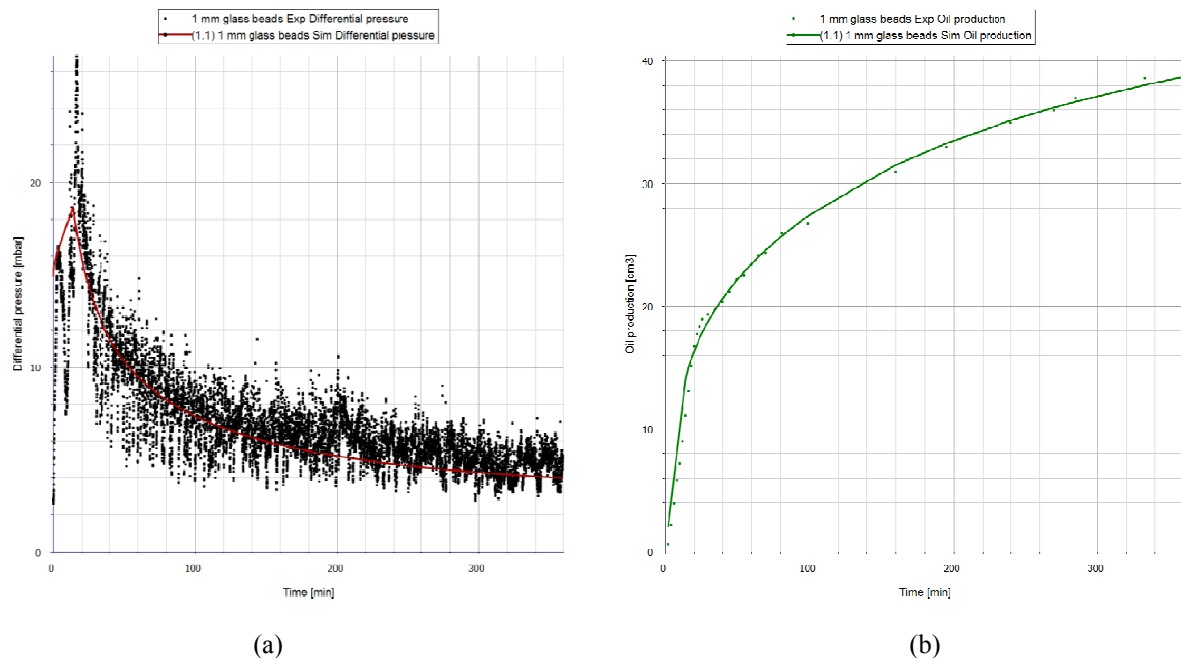


Figure 3. a) Differential pressure data match for experiment LT at 70°C; b) Production curve match for experiment LT at 70 °C. Dots show the experimental data and the continuous lines show the simulation match

The relative permeabilities based on these matches are shown on Figure 4 and compared with 50°C experiment. As shown on this figure the end points are shifted and the permeability curves are also different for the two cases.

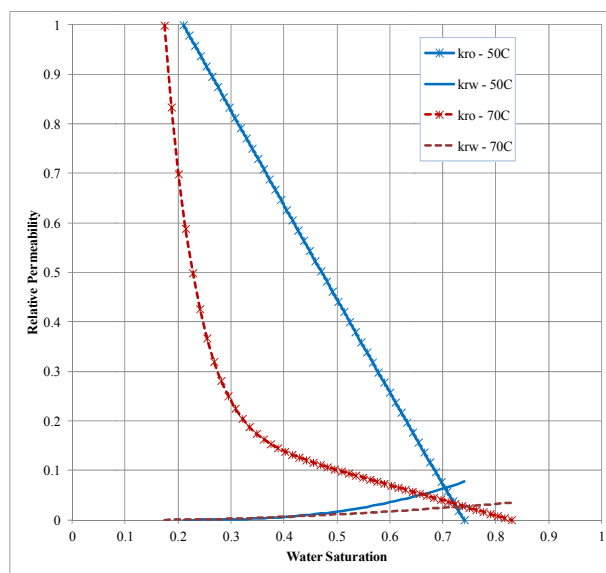


Figure 4. Relative permeability for LT experiments

The relative permeability curves for HT experiments done on 1 mm glass beads (GBs) using OIL20 are shown on Figure 5. These curves are shown on Figure 5b as normalized relative permeability curves. Both water saturation and relative permeabilities are normalized on Figure 5b to only show the difference in curvature of the data. Both high temperature and low temperature relative permeabilities show some variations by temperature. However, no direct conclusion can be drawn at this point.



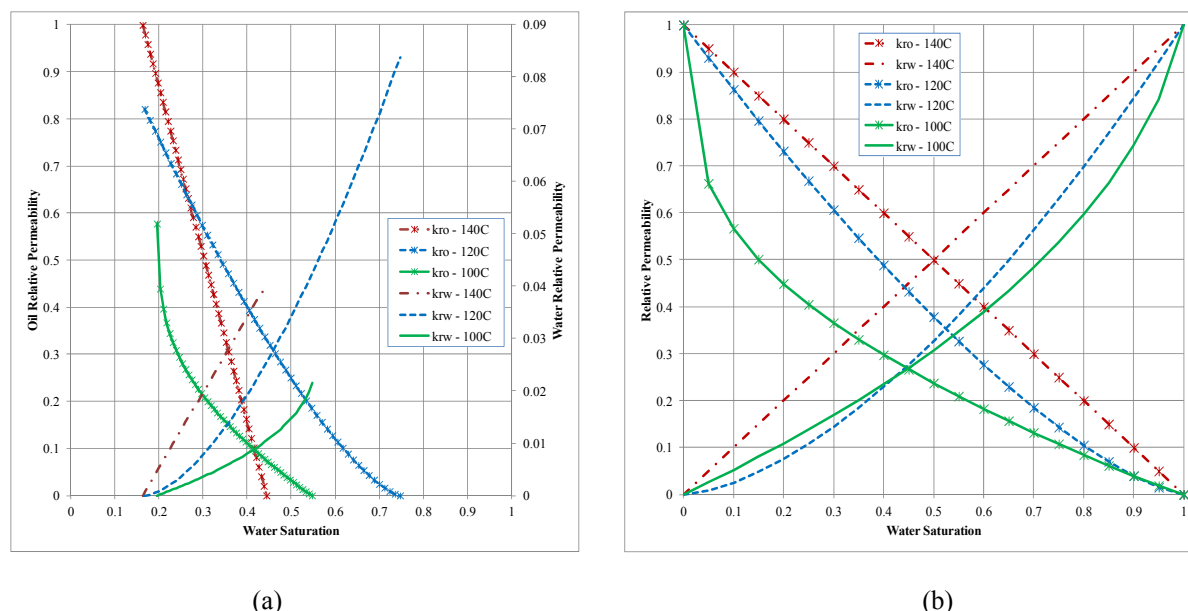


Figure 5. Relative permeability curves for HT experiments done on 1 mm GBs using OIL20. Normalized values are shown on Figure (b)

The experiment at 120°C was done twice injecting water at different rates. The effect of injection rate on production curves is revealed in Figure 6. As seen in this figure the ultimate recovery is almost the same. However, higher injection rate results in faster recovery. Figure 7 compares the relative permeability data for these two experimental runs. The initial water saturation and residual oil saturation values did not change significantly. The relative permeability curves, however, showed injection rate dependency. The values for oil seemed to be increasing while water relative permeability decreased as the injection rate increased. The relative permeability curves obtained for the HT experiments on 1 mm GBs media using OIL10 are shown in Figure 8 with the normalized values on the part (b) of the figure. Note that the values of water relative permeability are magnified for better visibility on Figure 8a.

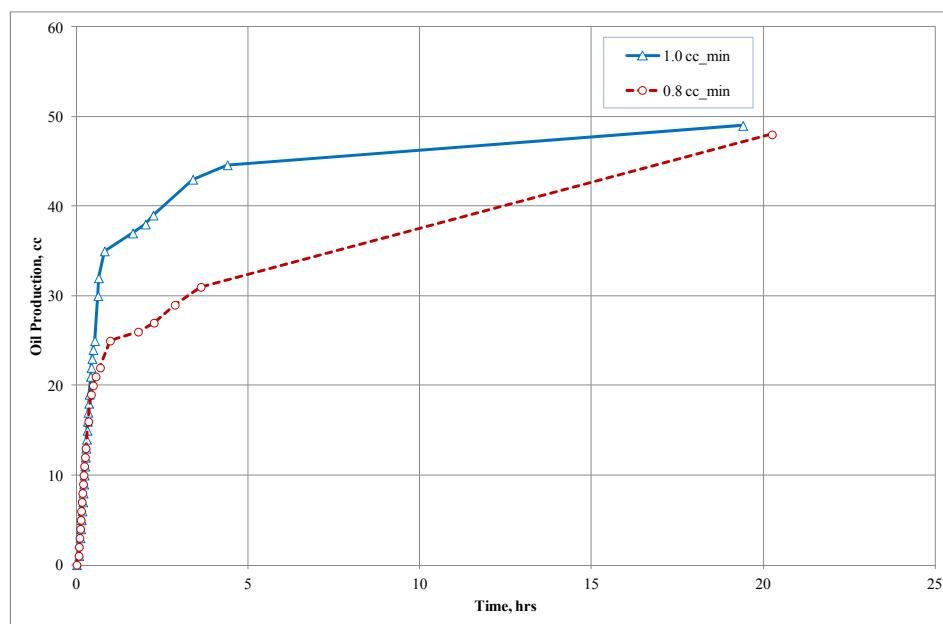


Figure 6. Oil production curves for HT experiments at 120°C (1 mm GBs, OIL20) showing the effect of water injection rate

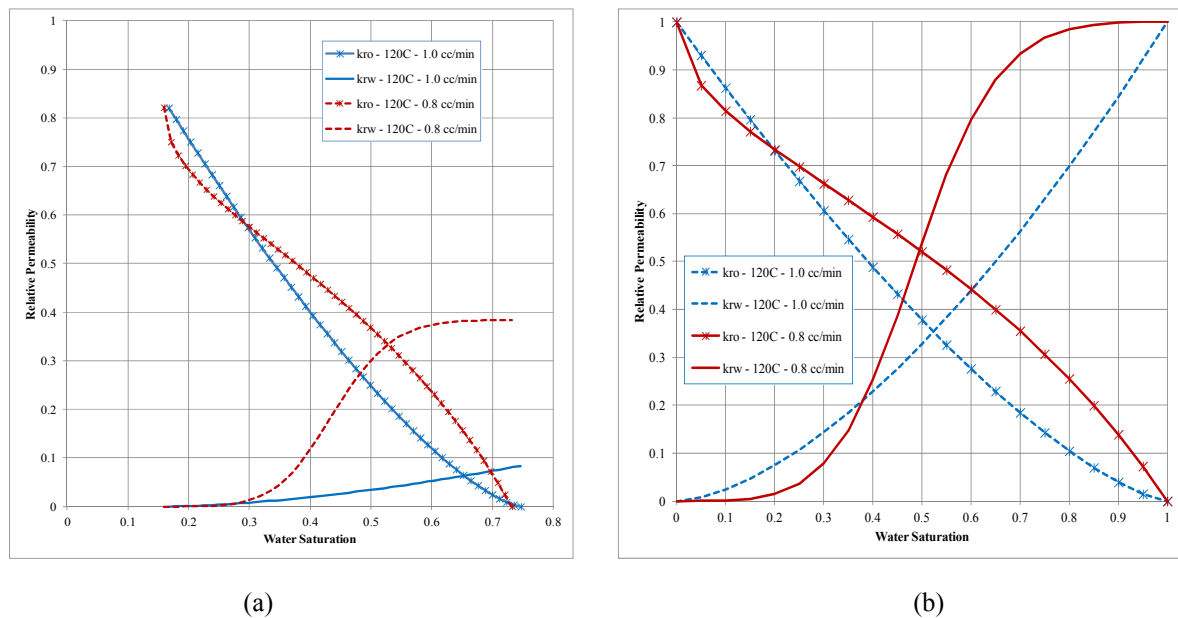


Figure 7. Relative permeability curves showing the effect of water injection rate. Normalized values on Figure (b)

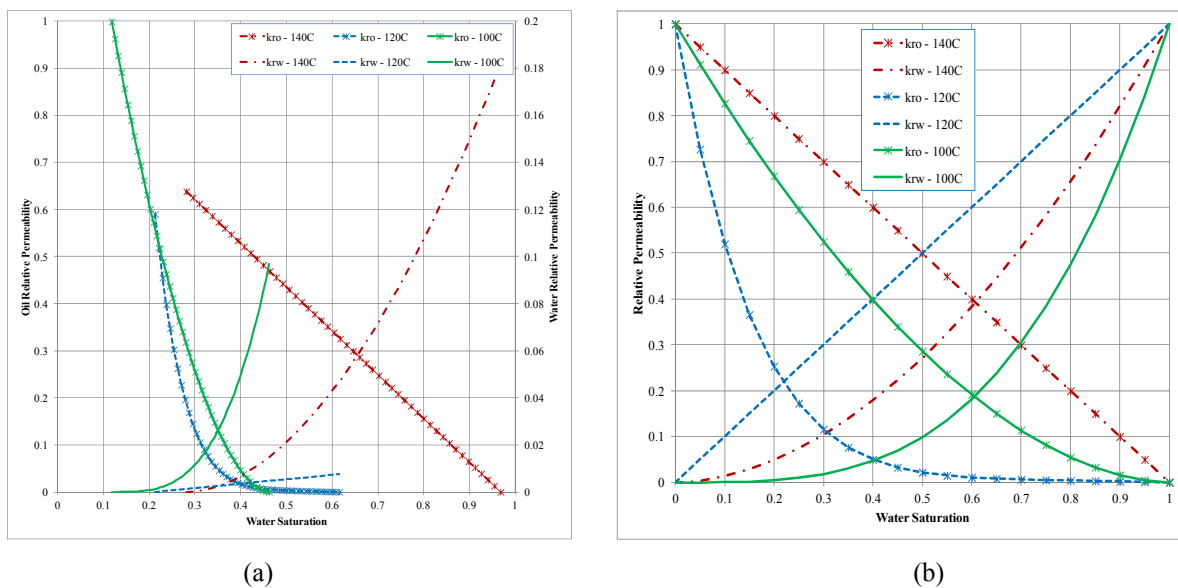


Figure 8. Relative permeability curves for HT experiments done on 1 mm GBs using OIL10. Normalized values are shown on Figure (b)

The same experiments, done using glass beads of smaller size as the porous media, have resulted in almost the same set of relative permeability curves. There seems not to exist a unique trend and definite dependency on temperature, as the curves have sometimes increased from one temperature to another and then decreased as the temperature has further been increased. The relative permeability curves obtained for HT experiments on 300-425 micron size GBs using OIL10 are shown on Figure 9. Part (a) of the figure shows normal plots of relative permeability versus water saturation. In part (b), however, normalized relative permeability values are plotted against normalized water saturation. Part (c) of the figure shows semi-log plots for two temperatures, namely 120°C and 140°C.

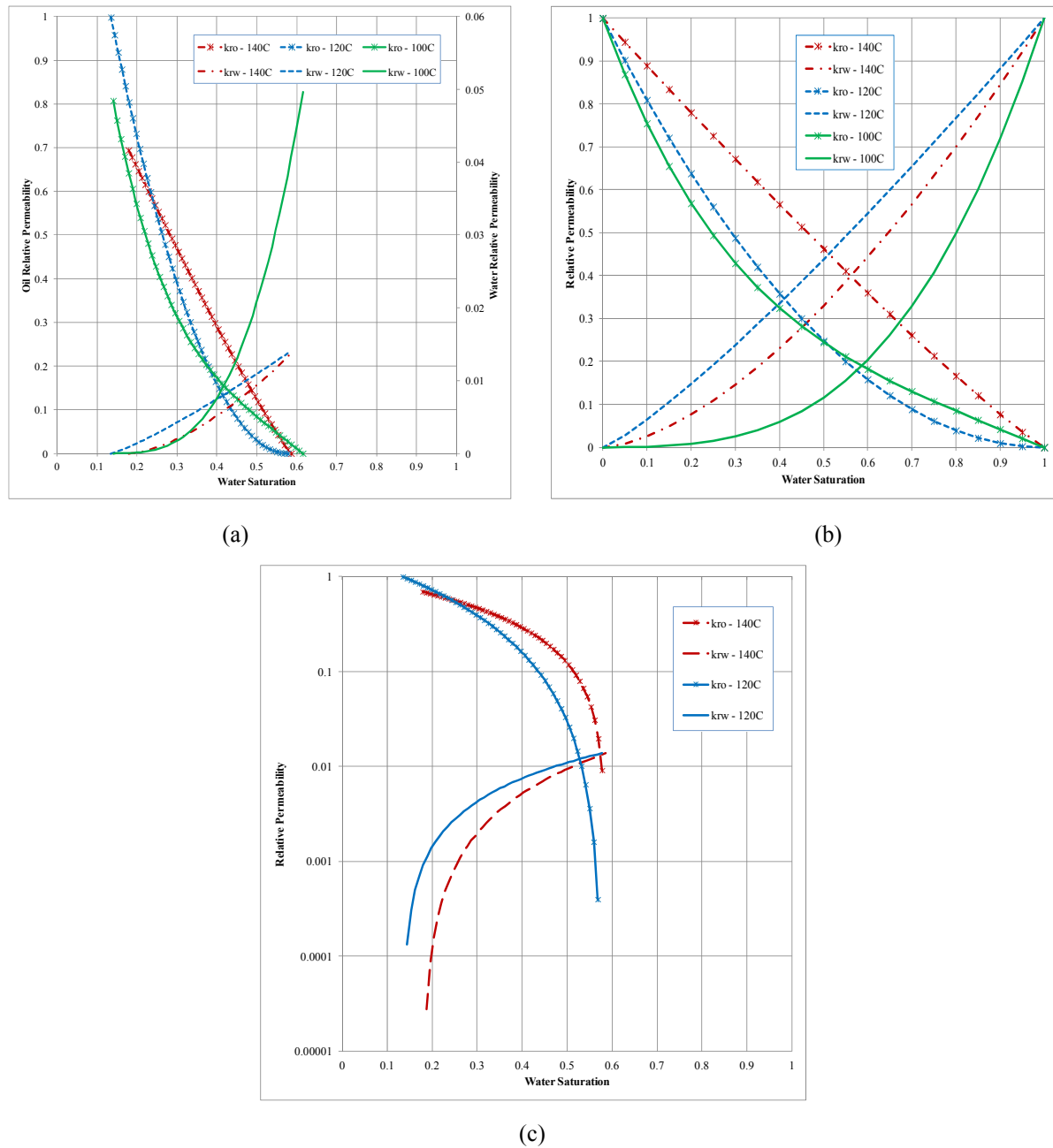


Figure 9. Relative permeability curves for HT experiments done on 300-425 micron GBs using OIL10. Normalized values are shown on Figure (b) Semi log curve for 120°C and 140°C on Figure (c)

HT experiments performed using OIL20 on the smaller sized GBs, namely 300-425 micron, have been analyzed and the resulting relative permeability curves are revealed in Figure 10.

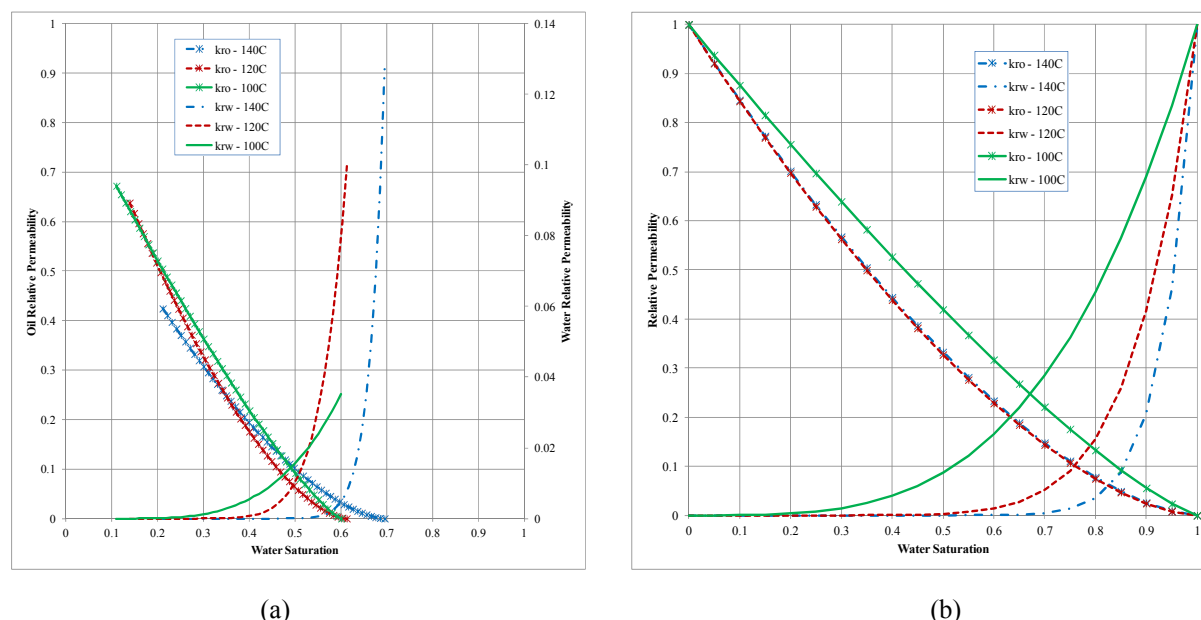


Figure 10. Relative permeability curves for HT experiments done on 300-425 micron GBs using OIL20. Normalized values are shown on Figure (b)

The increase of initial water saturation ( $S_{wi}$ ) versus temperature has been spotted generally, although not present in all the experimental results. We believe in those experiments we might have been inside the experimental error margin. But generally the increase in  $S_{wi}$  as the temperature increases is expected, as the oil viscosity drops much more than water viscosity. As the result the viscosity ratio of water to oil increases and will result in an unfavorable displacement of water by oil during initialization of core. During the water flooding of oil saturated core, the same interpretation should apply regarding the residual oil saturation ( $S_{or}$ ). As the temperature increases the viscosity ratio of oil to water drops, and this results in a more favorable mobility ratio and  $S_{or}$  is expected to decrease. However, this was not the case in some of the experiments. We think this could have happened due to viscous instabilities and possible viscous fingering in core flooding experiments. Viscous fingering seems to be inevitable in such an adverse mobility ratio condition, even at low injection rates.

As per the effect of temperature on relative permeability curves, we were not able to determine a unique trend in our experimental results. Dependency of either oil or water relative permeability on temperature is not justified in any of the experiments performed. The spread in relative permeability variation by temperature is even more adverse in the tests with higher permeable GBs (1 mm size). This further suggests that the variations seen can be attributed to viscous instabilities. This has also been reported by several authors. Sufi et al. (1982) and Miller and Ramey (1985) have concluded that the variations in relative permeability with temperature are probably not related to fundamental flow properties and they are rather related to experimental artifacts. Polikar et al. (1990) also stated that it is not possible to predict theoretically what the effect of temperature on relative permeabilities could be, and the results are system specific. Maini and Okazawa (1987) have also concluded that due to several artifacts involved in the experiments no effect of temperature could be justified.

## 5. Conclusions

In this work, laboratory core flooding experiments were conducted on Athabasca type oil with varying viscosities and using glass bead packs of different size as the porous media. Our aim was to investigate any possible effect of temperature on the oil and water relative permeability curves during imbibitions of water in the cores. For this purpose the oil production curves and the pressure drop across the core were history matched using Sendra core flooding simulator. This simulator acts as an optimization tool to help adjust the relative permeability correlation parameters and come up with the best curves that can match the laboratory measured data. The following conclusions can be drawn from this experimental investigation.

- 1) The increase of initial water saturation ( $S_{wi}$ ) versus temperature has been spotted generally, although not present in all the experimental results. We believe in those experiments we might have been inside the experimental error margin.

- 2) The decrease in residual oil saturation ( $S_{or}$ ) versus temperature has been observed. However, this was not the case in some of the experiments. We think this could have happened due to viscous instabilities and possible viscous fingering in core flooding experiments.
- 3) No dependency of either oil or water relative permeability on temperature is justified in any of the experiments performed. Not a unique increasing or decreasing trend could be seen versus the temperature. The spread in relative permeability variation by temperature is even more adverse in the higher permeable tests. This further suggests that the variations seen can be attributed to viscous instabilities.
- 4) The changes seen in relative permeability curves at different temperatures are probably more related to experimental artifacts and fingering issues than fundamental flow properties. We should, however, mention that the conclusions drawn cannot apply in general, and the temperature dependency issue is quite case specific.

### Acknowledgements

We would like to thank Statoil ASA for providing financial support. We also thank Weatherford Petroleum Consultants AS for providing us the license to Sendra.

### References

- Abasov, M. T., Tairov, N. D., Abdullaeva, A. A., Alieva, Sh. M., & Mamedov, A. I. (1976). Influence of Temperature on Relative Phase Permeability at High Pressures. *Dokl. Akad. Nauk Azerb. SSR.*, 8, 31-34.
- Amyx, J. W., Bass, D. M., & Whiting, R. L. (1960). *Petroleum reservoir engineering: physical properties*. New York: McGraw-Hill.
- Ashrafi, M., Souraki, Y., Karimaie, H., Torsaeter, O., & Bjorkvik, B. J. A. (2011). Experimental PVT Property Analyses for Athabasca Bitumen. Paper CSUG/SPE 147064 presented at the Canadian Unconventional Resources Conference held in Calgary, Alberta, Canada, 15-17 November. <http://dx.doi.org/10.2118/147064-MS>
- Bennion, D. W., Moore, R. G., & Thomas, F. B. (1985). Effect of Relative Permeability on the Numerical Simulation of the Steam Stimulation Process. *JCPT*, 24(2), 40-44. <http://dx.doi.org/10.2118/85-02-01>
- Burdine, N. T. (1953). Relative Permeability Calculations from Pore Size Distribution. *Trans., AIME*, 198, 71-78.
- Chierici, G. L. (1984). Novel Relations for Drainage and Imbibition Relative Permeabilities. *SPEJ*, 275-276. <http://dx.doi.org/10.2118/10165-PA>
- Combarnous, M., & Pavan, J. (1968). *Displacement par l'eau chaude d'huiles en place dans un milieu poreux*. Communication no. 37, III Colloque A.R.T.F.P., pp. 737-757, Pau, Sep. 23-26 (in French).
- Corey, A. T. (1954). The Interrelation between Gas and Oil Relative Permeabilities. *Prod.*, 19(1), 38-41.
- Davidson, L. B. (1969). The Effect of Temperature on the Permeability Ratio of Different Fluid Pairs in Two-Phase Systems. *JPT*, 21(8), 1037-1046. <http://dx.doi.org/10.2118/2298-PA>
- Edmondson, T. A. (1965). Effect of Temperature on Waterfloodig. *Journal of Canadian Petroleum Technology*, 4(4), 236-242. <http://dx.doi.org/10.2118/65-04-09>
- Honarpour, M., Koederitz, L., & Herbert, H. A. (1986). *Relative Permeability of Petroleum reservoirs*. C.R.C. Press Inc.
- Johnson, E. F., Bossler, D. P., & Naumann, V. O. (1959). Calculation of Relative Permeability from Displacement Experiments. *Trans. AIME*, 216, 370-372.
- Jones, S. C., & Roszelle, W. O. (1978). Graphical Techniques for Determining Relative Permeability from Displacement Experiments. *JPT*, 807-817. <http://dx.doi.org/10.2118/6045-PA>
- Khan, M. A. B., Mehrotra, A. K., & Svrcek, W. Y. (1984). Viscosity Models for Gas-Free Athabasca Bitumen. *J. Can. Pet. Tech.*, 23(3), 47-53. <http://dx.doi.org/10.2118/84-03-05>
- Lo, H. Y., & Mungan, N. (1973). Temperature Effect on relative Permeabilities and Residual Saturations. Research report RR-19, Petroleum Recovery Institute, Calgary, AB.
- Lomeland, F., Ebeltoft, E., & Thomas, W. H. (2005). A New Versatile Relative Permeability Correlation. Reviewed paper at the at the 2005 International Symposium of the SCA, August 21-25, 2005, Toronto, Canada. Retrieved from [http://www.scaweb.org/assets/papers/2005\\_papers/1-SCA2005-32.pdf](http://www.scaweb.org/assets/papers/2005_papers/1-SCA2005-32.pdf)
- Maini, B. B., & Batycky, J. P. (1985). The Effect of Temperature on Heavy Oil/Water Relative Permeabilities in

- Horizontally and Vertically Drilled Core Plugs. *JPT*, 37(8), 1500-1510. [http://dx.doi.org/ 10.2118/12115-PA](http://dx.doi.org/10.2118/12115-PA)
- Maini, B. B., & Okazawa, T. (1987). Effect of Temperature on Heavy Oil-Water Relative Permeability of Sand. *JCPT*, 26(3), 33-41. [http://dx.doi.org/ 10.2118/87-03-03](http://dx.doi.org/10.2118/87-03-03)
- Miller, M. A., & Ramey, H. J. Jr. (1985). Effect of Temperature on Oil/Water Relative Permeabilities of Unconsolidated and Consolidated Sands. *SPEJ*, 25(6), 945-953. [http://dx.doi.org/ 10.2118/12116-PA](http://dx.doi.org/10.2118/12116-PA)
- Polikar, M., Farouq Ali, S. M., & Puttagunta, V. R. (1990). High Temperature Relative Permeabilities for Athabasca Oil Sands. *SPEJ*, 5(1), 25-32. <http://dx.doi.org/10.2118/17424-PA>
- Poston, S. W., Ysrael, S., Hossain, A. K. M. S., Montgomery, E. F. III, & Ramey, H. J. Jr. (1970). The Effect of Temperature on Irreducible Water Saturation and Relative Permeability of Unconsolidated Sand. *SPE Journal*, 10(2), 171-180. [http://dx.doi.org/ 10.2118/1897-PA](http://dx.doi.org/10.2118/1897-PA)
- Schembre, J. M., Tang, G. Q., & Kovscek, A. R. (2006). Interrelationship of Temperature and Wettability on the Relative Permeability of Heavy Oil in Diatomaceous Rocks. *SPEJ*, 9(3), 239-250. <http://dx.doi.org/10.2118/93831-PA>
- Sedae, S. B., Rashidi, F., & Babadagli, T. (2007). Temperature Effects on the Heavy Oil/Water Relative Permeabilities of Carbonate Rocks. *Journal of Petroleum Science and Engineering*, 59, 27-42. <http://dx.doi.org/10.1016/j.petrol.2007.02.005>
- Sendra User Guide. (2012). Retrieved from <http://www.sendra.no>
- Sigmund, P. M., & McCaffery, F. G. (1979). An improved Unsteady-state Procedure for Determining the Relative Permeability Characteristics of Heterogeneous Porous Media. *SPEJ*, 19(1), 15-28. [http://dx.doi.org/ 10.2118/6720-PA](http://dx.doi.org/10.2118/6720-PA)
- Sinnokrot, A. A., Ramey, H. J. Jr., & Marsden, S. S. Jr. (1971). Effect of Temperature Level on Capillary Pressure Curves. *SPE Journal*, 11(1), 13-22. [http://dx.doi.org/ 10.2118/2517-PA](http://dx.doi.org/10.2118/2517-PA)
- Sufi, A. H. (1982). *Temperature Effects on Oil-Water Relative Permeabilities for Unconsolidated Sands*. PhD Thesis, Stanford University, Stanford, CA.
- Torabzadeh, S. J., & Handy, L. L. (1984). The Effect of Temperature and Interfacial Tension on Water/Oil Relative Permeabilities of Consolidated Sands. SPE/DOE 12689, 4th Symposium on EOR, Tulsa, OK, April 15-18. [http://dx.doi.org/ 10.2118/12689-MS](http://dx.doi.org/10.2118/12689-MS)
- Wang, J., Dong, M., & Asghari, K. (2006). Effect of Oil Viscosity on Heavy Oil/Water Relative Permeability Curves. SPE 99763, SPE/DOE Symposium on IOR, Tulsa, OK, April 22-26. <http://dx.doi.org/10.2118/99763-MS>
- Weinbrandt, R. M., Ramey, H. J. Jr., & Casse, F. J. (1975). The Effect of Temperature on Relative and Absolute Permeability of Sandstones. *SPE Journal*, 15(5), 376-384. [http://dx.doi.org/ 10.2118/4142-PA](http://dx.doi.org/10.2118/4142-PA)
- Wilson, J. W. (1956). Determination of Relative Permeability under Simulated Reservoir Conditions. *AIChE Journal*, 2(1), 94-100. [http://dx.doi.org/ 10.1002/aic.690020120](http://dx.doi.org/10.1002/aic.690020120)